

Handheld Erythema and Bruise Detector

Linghua Kong, Stephen Sprigle, Mark G. Duckworth, Dingrong Yi,
Jayme J. Caspall, Jiwu Wang*, Futing Zhao*

Center for Assistive Technology and Environmental Access, College of Architecture, Georgia
Institute of Technology Atlanta GA 30318 , USA

*Beijing Bodian Optical Technology Co. Ltd, 100026, China

ABSTRACT

Visual inspection of intact skin is commonly used when assessing persons for pressure ulcers and bruises. Melanin masks skin discoloration hindering visual inspection in people with darkly pigmented skin. The objective of the project is to develop a point of care technology capable of detecting erythema and bruises in persons with darkly pigmented skin. Two significant hardware components, a color filter array and illumination system have been developed and tested. The color filter array targets four defined wavelengths and has been designed to fit onto a CMOS sensor. The crafting process generates a multilayer film on a glass substrate using vacuum ion beam splitter and lithographic techniques. The illumination system is based upon LEDs and targets these same pre-defined wavelengths. Together, these components are being used to create a small, handheld multispectral imaging device. Compared to other multi spectral technologies (multi prisms, optical-acoustic crystal and others), the design provides simple, low cost instrumentation that has many potential multi spectral imaging applications which require a handheld detector.

INTRODUCTION — PURPOSE

Visual inspection of intact skin is a common means to identify and characterize bruising and erythema. In people with darkly pigmented skin, the presence of melanin greatly hinders visualization of discoloration. A need exists for clinically usable technology that assists clinicians in assessing dark skin.

Previous Bruise Detection Methods During investigations of potential child and elder abuse, clinicians and forensic practitioners assess bruises to document shape, extent and estimate age. Visual inspection in vivo and photography of bruises are two conventional methods employed in clinical practice. However they are qualitative, subjective, inaccurate and hence unreliable. Statistics indicate that their best accuracy is only about 50% [1-4]. Further, their failure rate is even much higher if bruises happened on darkly pigmented skin.

Recently spectroscopy has emerged to improve the reliability of bruise detection [5, 6]. It infers the fractional contents of various chromophores (oxy-hemoglobin (oxyHb), deoxy-hemoglobin (deoxyHb), bilirubin, melanin) by measuring the optical reflectivity of one sample point at a time of bruised region for a continuous range of wavelength at fine steps (e.g., at 2nm incremental step). It is a reliable tool to investigate the basic biochemical processes associated with bruised skin on both white and darkly pigmented skin. However, point spectroscopy can be too time consuming and tedious for clinical use since one must image multiple locations. Moreover, point spectroscopy is not conducive to create a distribution map of the chromophore concentration over time. Such a map is important since it contains the intrinsic features of the diseased skin such as its shape, size and age [7].

Previous Erythema Identification Methods Over the past decade, researchers have identified erythema identification using non invasive methods [8-10]. Additional studies [11, 12] analyzed erythema based on the changes in skin color using true color images. However, they did not report cases on darkly pigmented skin. Tissue Reflectance Spectroscopy (TRS) was clinically used to detect Stage I ulcers in subjects with different types of skin [13, 14]. They reported high sensitivity (85%) and specificity (75%). However, similar to the case of bruise detection, TRS is performed at one spatial point at a time which makes the practical clinical diagnostic procedure tedious, time consuming and laborious.

Multispectral Imaging Method and Applications Multi-spectral imaging has matured into a technology with many applications, including classification of difficult targets in defense [15], produce sorting [16], precision farming in agriculture [17], product quality online inspection in manufacturing [18], contamination detection in food industry [19], remote sensing in mining [20], atmospheric composition monitoring in environmental engineering, and early stage diagnosis of cancer and tumors [21-24]. With great progressive pace, multi-spectral imaging is replacing many visual or visual experience based diagnostic methods as the most important disease diagnostic tool and post treatment diagnostic tool (in medical imaging).

Both TRS and multispectral imaging methods measure light reflectivity of diseased skin. The difference is that the former samples more densely in the spectral domain and more sparsely over the spatial domain than the latter. Images of millions of samples (e.g. 600x800 pixels for a typical low-cost CCD camera) can be conveniently obtained at a set of discrete wavelengths using band pass filters to remove unimportant spectra. This makes a multi-spectral imaging system a cost effective and efficient tool for detecting and characterizing bruises and erythema. Results of initial efforts of using multi-spectral imaging to study erythema and cutaneous inflammation in vivo [25, 26] indicate that it allows for the construction of quantitative maps relating to erythema and edema.

The most extensive study of bruise age using indexes of bilirubin and hemoglobin over time were reported in Randeberg and colleagues [27]. They used multi-spectral imaging to detect and characterize bruises on light pigmented skin at spectral ranges of 400 – 1000nm (VNIR) and 900 – 1700nm (SWIR). However they did not report using this approach on darkly pigmented skin.

Current multispectral imaging applications require either multiple exposures or extensive post-processing. Examples of these current technologies include filter wheels, generalized Lyot filter, electrical tunable filter, optic-acoustic based SmartSpectra, NASA's Multi Spectral Imager. These devices are not well suited for point of care applications with respect to durability, portability and cost.

This paper describes the design and development of the key components required of a handheld multispectral imager. A mosaic filter has been developed containing four filters synchronized to chromophores of interest in bruise and erythema detection. As a companion to this filter, an illumination system has been developed that bathes the area of interest with light consisting of the same wavelengths targeted by the mosaic filter.

PRELIMINARY INVESTIGATION

The initial aspect of this research characterized bruising and erythema using a multispectral imaging system based upon a filter wheel. This work identified a small set of filters that provide needed spectral information and fusion algorithms to achieve contrast enhancement [5, 6].

Using these findings, we focused attention on hardware compatible with the goal of developing a handheld point-of-care device capable of detecting erythema and bruising in people with varying skin tones.

HARDWARE DESIGN

To realize a point-of-care clinical tool, the underlying technology had to overcome significant usability barriers: device cost, imaging using a single exposure, adequate speed of image processing, and compatible with different clinical environments.

These requirements were met via the development of a custom filter mosaic and accompanying illumination system.

Custom filter mosaic.

The filter design was based those used within CMOS technology. CMOS offers adequate technical performance at low cost and is easily integrated with board-level electronics. CMOS cameras utilize a color filter array, i.e. Bayer filter, consisting of red, green and blue filters that sits atop the sensing elements giving a wide band transmission profile. Images are reconstructed from a mosaic filter arrangement. Current cameras reconstruct from 3 filters, but in reality, the filter array element reflects a 4 element mosaic having twice as many green elements as red or blue. Therefore, our filter design was based upon a four element mosaic with two significant differences from Bayer filters: the mosaic uses narrow band filters and these filters are tuned specifically to chromophores of interest.

The design is illustrated in Figure 1 and results in a narrow band spectral response synced to four defined wavelengths. The initial versions of the device focus on spectra related to bilirubin, hemoglobin and water. Multiple filters have been developed that use four filters center on five possible filters 460nm, 525nm, 577nm, 650nm, and 970nm.

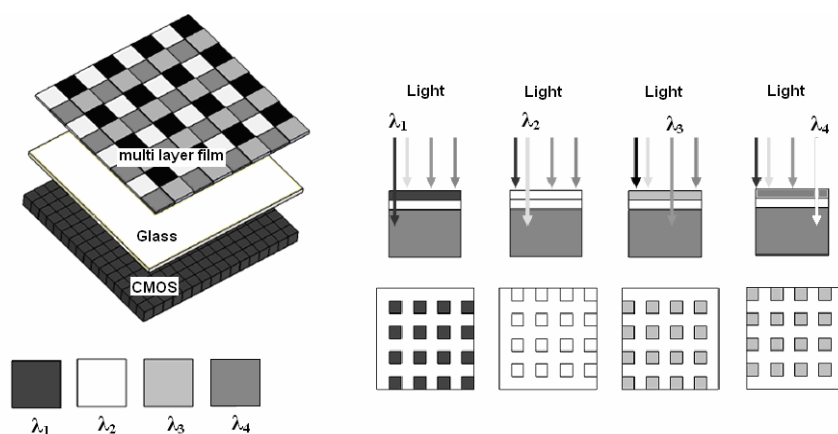


Figure 1 Four element color filter array

Image resolution is important to distinguish spatial relationships of chromophores. We have defined the minimum area of interest as 1 sq mm, requiring the need to ‘sample’ at 0.5 mm. Given a target size of 10 cm x 10cm, and a required resolution of 0.5 mm, an element will require 200 x 200 pixels or a total of 160,000 pixels for a 4 filter array. This results in the requirement to fabricate a mosaic based upon $\approx 20.8 \mu\text{m}$ square filters to be compatible with existing CMOS sensors.

Compatibility with existing CMOS sensors permits use of commercial chips, thereby meeting the requirement to control device costs. The mosaic design permits creation of a multispectral image using a single exposure. Finally, because no image registration is required, processing can occur rapidly. Therefore, this conceptual design met the major design criteria established for the clinical device. The major technological hurdles, however, lay in fabrication.

Crafting process of fabricating custom mosaic filter

The crafting process generates a multilayer film on a glass substrate using vacuum ion beam splitter and lithographic techniques. The mosaic filter array can be fabricated on any substrate, provided that the substrate does not interfere substantially or materially affect performance of the filter array. In the current design, the mosaic filter was fabricated on a glass substrate.

The glass substrate should be approximately 0.3 mm to approximately 0.5 mm thick. The mosaic filter disposed on the substrate can then be laminated on the surface of a photosensor, such as a CMOS sensor or disposed on a layer of 0.1 mm thick glass on the surface of a photosensor sensor.

Precisely-shaped masks are necessary for fabricating filter film structures at a designated position on the substrate. The masks are fabricated by optical lithography technology. In order to fabricate filter mosaic, at least four (4) kinds of masks are needed, which can both prevent the transmittance of ultraviolet (UV) light and can project a selected geometry onto a substrate.

First, a photoresist compound is applied to coat a clean substrate, (e.g., glass). Following solidification of the photoresist, the first mask is applied to the substrate. The masked substrate is then exposed to an UV light environment. After exposure of the masked substrate to UV light, the portions of the photoresist that were exposed to UV light are removed by liquid erosion to reveal the underlying substrate. The remaining photoresist that was unexposed to UV light forms the first mask for deposition. This optical lithography process is repeated until the at least four kinds of masks are fabricated onto the substrate (Figure 2).

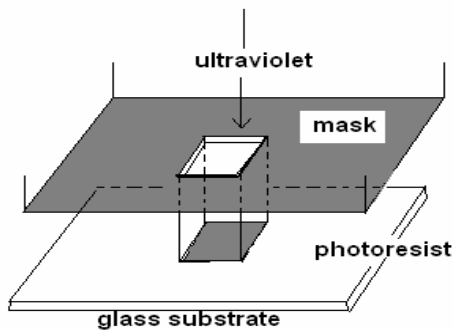


Figure 2 Masking using repeated lithographic process

Upon completion of the optical lithography process, deposition of multi-layer thin films are performed by the process of physical vapor deposition (PVD) within a vacuum chamber. Multi-layer thin films are constructed by sandwiching at least three (3) kinds of coating materials (TiO₂, Al₂O₃, and Ag) to form an optical thin film system comprising approximately twelve (12) layers with thicknesses ranging from 40 nm to 150 nm. The coating materials are heated by an electron beam gun to generate a vapor of the coating material within a vacuum chamber.

The pressure in the vacuum chamber ranges from approximately 0.01 Pascals (Pa) to approximately 0.02 Pa. The vapor of a coating material coagulates on the surface of the substrate to form a thin film. The substrate undergoing PVD is periodically bombarded by an argon (Ar) ion beam, which serves a dual function: removal of potential molecular layers of water that can accumulate on the substrate, and to activate the surface of the substrate, improving adhesion of the coating material to the substrate. In order to improve the environmental characteristics of the coatings, Ar ion bombardment is conducted throughout the deposition process to increase the density of the coating micro-configurations.

The thickness of each thin film layer system is monitored using a monochrome photometer. The accuracy of the monitoring of thin film thickness is determinative of the spectral properties of each thin film. The conditions of the PVD process can be varied depending upon the coating material used, the composition of residual gases within the deposition chamber (e.g., H₂O, N₂, O₂, H₂, and oil vapor), and the substrate temperature (approximately 80°C). The deposition rate, ranging from approximately 0.3 nm/s to approximately 2 nm/s, can also affect the performance of the coatings. The PVD process is repeated for each of the at least four (4) filters comprised of at least four (4) coatings to fabricate a mosaic filter.

Figure 3 shows a section of prototype mosaic filter for one set of wavelengths $\lambda = 540\text{nm}, 577\text{nm}, 650\text{nm}, 970$. The image shown here was taken from CCD microscope. Subsequent improvements to the fabrication process have reduced the spacing (gap, border) between individual filters to 1 μm - 2 μm . Figure 4 shows the narrow band characteristics of the mosaic.

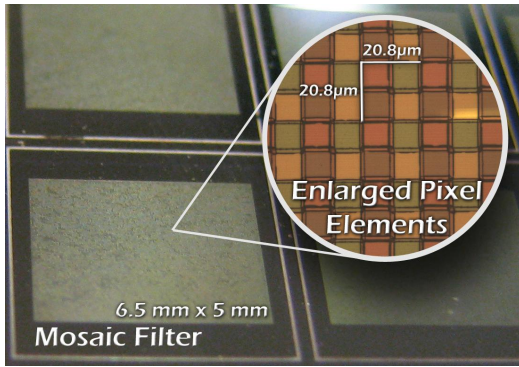


Figure 3 A section of prototype mosaic filter for one set of wavelengths

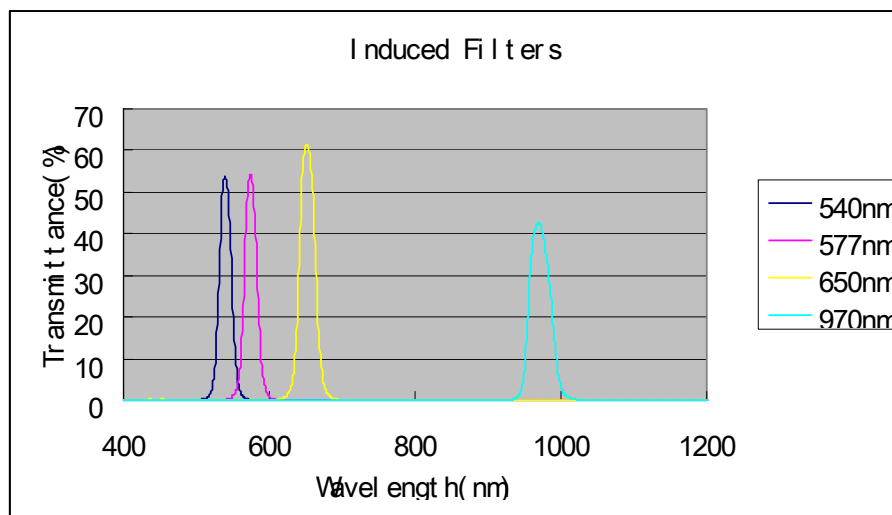


Figure 4 Transmittance of a set of four featured wavelengths through the filter array

Illumination system. One challenge in creating a clinical multispectral instrument is the variable ambient lighting conditions. For the mosaic filter to work properly, the clinical target must be bathed in light that contains the spectra of interest. In addition, lighting requirements must be compatible with the portability requirements of a handheld device. Specifically, we desired a battery-operated device that can be carried in a lab coat, so size and weight were important considerations.

To overcome these potential barriers, we designed and fabricated a LED-based illumination. LEDs are low cost, have low power requirements and permit the light source to be tuned for the application- in this case- tuned to the wavelengths of interest. Each type of LED is powered by a constant voltage supply circuit which helps independently adjust the intensity of these four colors in order to compensate for differences in radiated power distribution. The design used as test bed can work at a nominal voltage of 13.5V, 1.7A with a maximum power consumption of 23W and 600 lux peak illumination and 405 lux as average at a distance of 45cm. The next design iteration will operate at 5V, 5W which will meet the requirements for a handheld detector.

Figure 5 illustrates the prototype design and its spectral response that indicates its ability to bathe the target with light covering the spectrum of interest. The 940 nm LED is not shown due to the limitations of the spectrometer used to test the illumination system.

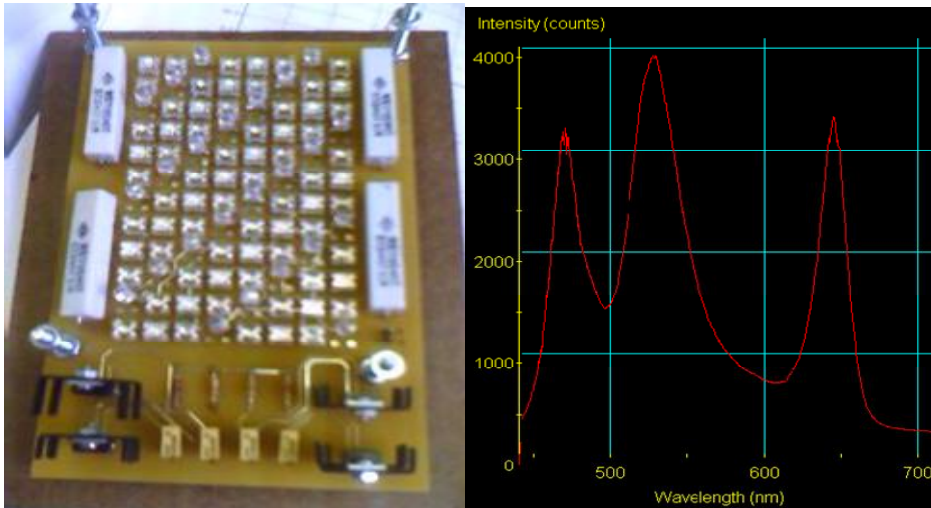


Figure 5 Prototype LED illumination system and an illustrated spectral power distribution.

BREAKTHROUGH POINTS

The use of a custom filter array overlaying a CMOS sensor represents a novel approach to multi spectral imaging. Compared to other multi spectral technologies (multi prisms, optical-acoustic crystal and others), the design provides simple, low cost instrumentation that has many potential multi spectral imaging applications which require a handheld detector.

The primary commercial benefits of the new technology are cost and size. This technology can be used to create small handheld multispectral devices at affordable costs. The real-time imaging process permits the design of devices capable of working in the field or at the point of care.

CONCLUSION

A custom filter mosaic and companion illumination system has been designed for use within a handheld clinical device. The mosaic is configured to be compatible with existing CMOS sensors, a design feature consistent with our targeted price point of \$500 cost of goods. The spectral characteristics of the mosaic and illumination system were designed to detect erythema and bruising, especially in persons with darkly pigmented skin.

The technology has other potential applications in biomedical and industrial imaging, including:

- spectral imaging of wounds to detect bioburden, infection, or necrosis
- spectral imaging of skin to quantify pathology including jaundice, dermatitis
- field imaging of produce to quickly identify bruises or discoloration
- monitoring poultry and plant disease in agriculture
- quality control in assembly line in many (e.g. semi conductor, pharmacy) industries, etc..

H. Literature cited

1. Bariciak, E.D., et al., *Dating of Bruises in Children: An Assessment of Physician Accuracy*. Pediatrics, 2003. **112**(4): p. 804-807.
2. Choi, S., et al., *Bruises Literature Review*. 2002, Children and Family Research Center, School of Social Work, University of Illinois at Urbana-Champaign: Urbana, Illinois. p. 17.
3. Maguire, S., et al., *Can you age bruises accurately in children? A systematic review*. Arch Dis Child, 2005. **90**(2): p. 187-189.

4. Schwartz, A.J. and L.R. Ricci, *How accurately can bruises be aged in abused children? Literature review and synthesis*. Pediatrics, 1996. **97**(2): p. 254-257.
5. Randeberg, L.L., *Diagnostic applications of diffuse reflectance spectroscopy*, in *Department of Electronics and Telecommunications*. 2005, Norwegian University of Science and Technology: Trondheim. p. 62.
6. Randeberg, L.L., et al., *A novel approach to age determination of traumatic injuries by reflectance spectroscopy*. Lasers in Surgery and Medicine, 2006. **38**(4): p. 277-289.
7. Stamatas, G.N., et al., *Non-invasive measurements of skin pigmentation in situ*. Pigment Cell Res, 2004. **17**(6): p. 618-26.
8. Chung, D.H. and G. Sapiro, *Segmenting skin lesions with partial-differential-equations-based image processing algorithms*. Medical Imaging, IEEE Transactions on, 2000. **19**(7): p. 763-767.
9. Maglogiannis, I., S. Pavlopoulos, and D. Koutsouris, *An integrated computer supported acquisition, handling, and characterization system for pigmented skin lesions in dermatological images*. Information Technology in Biomedicine, IEEE Transactions on, 2005. **9**(1): p. 86-98.
10. Zhang, J., et al., *A feasibility study of multispectral image analysis of skin tumors*. Biomedical Instrumentation & Technology, 2000. **24**(4): p. 275-282.
11. Hance, G.A., et al., *Unsupervised color image segmentation: with application to skin tumor borders*. Engineering in Medicine and Biology Magazine, IEEE, 1996. **15**(1): p. 104-111.
12. Nischik, M. and C. Forster, *Analysis of skin erythema using true-color images*. Medical Imaging, IEEE Transactions on, 1997. **16**(6): p. 711-716.
13. Riordan, B., S. Sprigle, and M. Linden, *Testing the validity of erythema detection algorithms*. Journal of Rehabilitation Research and Development, 2001. **38**(1): p. 13-22.
14. Sprigle, S., M. Linden, and B. Riordan, *Characterizing reactive hyperemia via tissue reflectance spectroscopy in response to an ischemic load across gender, age, skin pigmentation and diabetes*. Medical Engineering & Physics, 2002. **24**(10): p. 651-661.
15. Gat, N., *Full Stokes Vector Extraction with Imaging Spectro-Polarimetry Using a Liquid Crystal Tunable Filter and a Liquid Crystal Variable Retarder (LC-TF/VR)*. in *Detection & Classification of Difficult Targets*. 2002, US Army Aviation & Missile Command; Redstone Arsenal, Alabama.
16. Chen, Y.-R., K. Chao, and M.S. Kim, *Machine vision technology for agricultural applications*. Computers and Electronics in Agriculture, 2002. **36**: p. 173-191.
17. Shearer, S.A., Payne, F.A., *Color and Defect Sorting of Bell Peppers using Machine Vision*. Trans. ASAE, 1990. **33**(6): p. 2045-2050.
18. Pietikainen, M. and L.F. Pau, *Machine vision and advanced production*. Machine perception and artificial intelligence vol. 22. 1996, Hackensack, NJ: World Scientific
19. Carrasco, O., et al. *Hyperspectral imaging applied to medical diagnoses and food safety*. 2003: SPIE.
20. Spencer, C.H., *Remote sensing provides high-tech clues for mineral exploration*. 1998, Bio-Geo-Recon.
21. Gao, X., et al., *In vivo cancer targeting and imaging with semiconductor quantum dots*. Nat Biotechnol, 2004. **22**(8): p. 969-76.
22. Gebhart, S.C., W.-C. Lin, and A. Mahadevan-Jansen. *Characterization of a Spectral Imaging System*. in *Proceedings of SPIE: Spectral Imaging: Instrumentation, Applications, and Analysis II*. 2003: SPIE.
23. Jaganath, R., et al., *Diagnostic classification of urothelial cells in urine cytology specimens using exclusively spectral information*. Cancer, 2004. **102**(3): p. 186-91.
24. Mansfield, J.R., et al., *Near infrared spectroscopic reflectance imaging: a new tool in art conservation*. Vibrational Spectroscopy, 2001. **28**(1): p. 59-66.
25. Stamatas, G.N., C.J. Balas, and N. Kollias. *Hyperspectral image acquisition and analysis of skin*. in *Proceedings of SPIE: Spectral Imaging: Instrumentation, Applications, and Analysis II*. 2003: SPIE.
26. Stamatas, G.N. and N. Kollias. *Noninvasive quantitative documentation of cutaneous inflammation in vivo using spectral imaging*. in *Proceedings of SPIE: Photonic Therapeutics and Diagnostics II*. 2006: SPIE.
27. Randeberg, L.L., et al. *Hyperspectral imaging of bruised skin*. in *Proc. SPIE Vol. 6078: Photonic Therapeutics and Diagnostics II*. 2006.